DOI: 10.1002/zaac.201300641

Synthesis, Structure, and Luminescent Properties of Three Coordination Compounds Based on *in situ* Generated Tetrazolate and Carboxylate Ligands

Huiqing Ma,[a] Yuwen Xu,[b] Qingguo Meng,[a,c] Liangliang Zhang,*[b] Rongming Wang,[b] and Daofeng Sun*[a,b]

Keywords: X-ray diffraction; One-pot synthesis; *In situ* reaction; Structure elucidation; Hydrogen bonding

Abstract. Three metal organic coordination compounds, namely, $\{[Cd_2(L1)_4]_2 \cdot 9H_2O\}_n$ (**1**), $\{[Zn(L1)_2 \cdot 2H_2O]_2 \cdot H_2O\}_n$ (**2**), and $[Cu(L2)_2]_n$ (**3**), [L1 = 3-chloro-2-(5*H*-tetrazol-5-yl)pyridine; L2 = 3-chloropicolinic acid], were hydrothermally synthesized, in which L1 and L2 were synthesized by *in situ* reactions. X-ray diffraction analyses revealed that the 2D layer of complex **1** is built from a dinuclear Cd^{II} second building blocks, whereas complex **2** shows 0D structure, which is built based on two L1 ligands, one zinc ion, and two water molecules. **3** shows a 1D infinite rod-shaped chain. Additionally, the solid-state fluorescence properties for compound **1** and **2** are also presented.

1 Introduction

The construction of metal organic coordination compounds (MOCCs) have attracted much attentions over the past several decades for their intriguing topologies and potential applications in molecular selection, ion exchange, adsorption, fluorescence, catalysis, magnetism, and so on.[1–3] Except the well-known carboxylate ligands, N-heterocyclic bridging ligands such as imidazolate, pyrazolate, triazolate, and tetrazolate moieties have emerged as a unique class of building subunits. In particular, tetrazole-based ligands have attracted significant interest because of their variety of bridging modes, excellent coordination capacities, and potential applications in advanced materials.[4–8] In addition, the five-membered heterocyclic ring could also serve as a hydrogen-bond acceptor, thus permitting the polymeric framework to be expanded through hydrogen-bonding interactions.[9]

It is well known that compounds with CN groups can be easily transformed to organic carboxylates or tetrazole-based ligands via *in situ* reactions.[10] From a design perspective, the rapidly developing *in situ* ligand reaction may provide a new strategy in construction of functional metal organic coordination polymers.[11] 5-Aromatic group substituted-1*H*-tetrazoles are a class of rich organic compounds with labile coordination fashions, and their metal compounds should display excellent photoluminescent properties due to the high conjugacy of the tetrazolyl and phenyl group.[12] Thus, the weak forces, such as hydrogen and halogen bonds, π···π interactions, are also be considered, because they were suggested to act as a structure-direction tool.[13] Encouraged by these investigations, 3-chloro-2-cyanopyridine (L) was chosen as a precursor to construct coordination compounds via *in situ* reaction (Scheme 1).

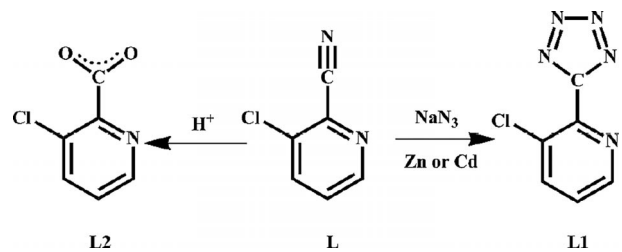

Scheme 1. Schematic representation of the organic ligands generated from *in situ* reaction.

In 2001, *Sharpless* and co-workers[14] reported a safe, convenient, and environmentally friendly procedure for the synthesis of a variety of 5-substituted 1H-tetrazoles in water. The 1H-tetrazoles are prepared by addition of azide to nitriles in water with zinc salts as Lewis acid catalysts. In this paper, as part of an ongoing program on hydrothermal reactions, we not only repeated the Demko-Sharpless reaction under hydrothermal conditions, but also successfully got compounds **1** and **2**, in which the precursor of tetrazole ligands and metal salt is

* Dr. L. Zhang
E-Mail: liangliangzhang@upc.edu.cn
* Prof. Dr. D. Sun
E-Mail: dfsun@sdu.edu.cn
[a] Key Lab for Colloid and Interface Chemistry of Education Ministry
School of Chemistry and Chemical Engineering
Shandong University
Jinan, P. R. China
[b] College of Science
China University of Petroleum (East China)
Qingdao Shandong, P. R. China
[c] Chemistry & Chemical and Environmental Engineering College
Weifang University
Weifang Shandong 261061, P. R. China
Supporting information for this article is available on the WWW under **http://dx.doi.org/10.1002/zaac.201300641** or from the author.

Zeitschrift für anorganische und allgemeine Chemie ZAAC Journal of Inorganic and General Chemistry

taken in the same 4:15 ratio (Scheme 1), and compound **3**, based on the hydrolysis reaction of cyanide with hydrochloric acid as catalysts (Scheme 2). For **1**, the Cd salt is a Lewis acid catalyst and for **2**, the Zn salt is a Lewis acid catalyst. In **1**, the ligand adopts μ3-bridging coordination mode and expands the dinuclear SBU into a 2D layer. But in **2**, the ligand adopts bidentate-chelate coordination mode and the coordinated water molecules in each Zn^{2+} ion prevent the dinuclear SBU further extension to form high dimensional framework. So the precursor of tetrazole ligand and metal salt is taken in the same 4:15 ratio in compound **1** and **2**, but the stoichiometries in compound **1** and **2** reveal the reverse trend.

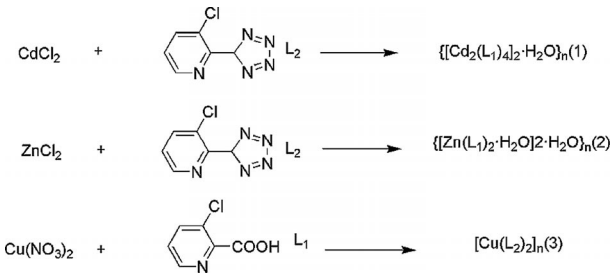

Scheme 2. Schematic representation of the coordination compounds generated from *in situ* reaction.

2 Results and Discussion

2.1 Crystal Structure of {[Cd$_2$(L1)$_4$]$_2$·9H$_2$O}$_n$ (1)

X-ray single crystal structure analysis reveals that complex **1** crystallizes in the monoclinic $P2_1/c$ space group. The asymmetric unit of **1** contains of one Cd^{II} atom and two L1 ligands. The coordination environment of the cadmium ion in **1** is shown in Figure 1. The Cd1 ion adopts a distorted octahedral arrangement, which is six-coordinate by six nitrogen atoms from four different L1 ligands. The Cd–N bond lengths range from 2.280(2) to 2.2647(19) Å, which are comparable with those previously reported Cd^{II} complexes based on tetrazole-based ligands.[15] In complex **1**, Cd1 and symmetry-related Cd1^a are connected by two L1 ligands to form the dinuclear SBU (Figure 1a). In the dinuclear SBU, the L1 ligand adopts *cis-cis* and *cis-trans* coordinated mode (Figure 1b). N5 and N7 atoms adopt bis-chelating bridging mode to link one cadmium atom and the N9 atom adopts mono-dentate coordination mode to link the other cadmium atom. Then, every *cis-trans* L1 ligand connects two dinuclear SBU and each dinuclear SBU attaches to four L1 ligands to result in the formation of a 2D layer (Figure 1c). The topological analysis of complex **1** was performed using OLEX.[16] If the dinuclear SBU is considered as a single node and the L1 ligand as a linear linker and the structure of compound **1** can be simplified to 4^4 layer[17] as shown in Figure 1d. Finally, two layers are interacted together through layer-to-layer hydrogen-bonding to generate a 3D non-porous supramolecular architecture.

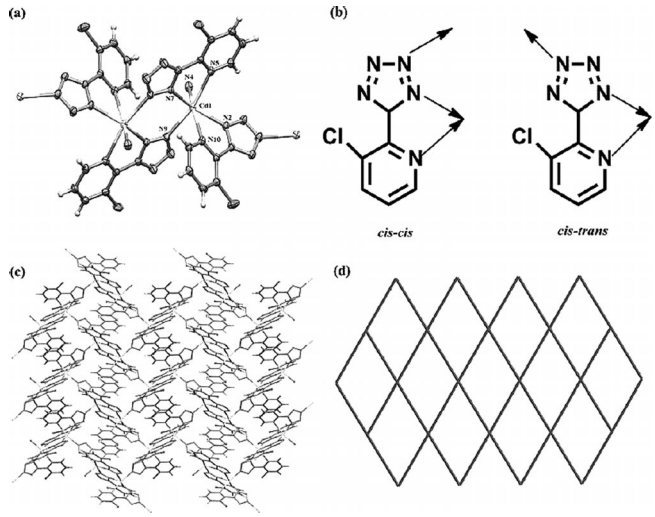

Figure 1. (a) Coordination environment of the Cd^{II} ion in complex **1**. (b) Coordination modes of L1 ligand. (c) 2D layer of complex **1**. (d) Schematic representation of the 4^4 topology framework of **1**.

2.2 Crystal Structure of {[Zn(L1)$_2$·2H$_2$O]$_2$·H$_2$O}$_n$ (2)

The single-crystal X-ray study of compound **2** exhibits a 0D structure constructed by the connection of zinc atom, two L1 ligands and two coordinated H_2O molecules. Compound **2** crystallizes in the triclinic space group $P\bar{1}$ (Figure 2a). Each central zinc atom adopts an octahedral arrangement and is bound by four nitrogen atoms from two different L1 molecules and two oxygen atoms from coordinated H_2O molecules. Two of L1 ligands act as the bidentate chelator and combine one zinc atom together to form the single nuclear zinc unit. The Zn–N bond lengths range from 2.113(2) to 2.154(2) Å, corresponding to the typical values in Zn^{II}-nitrogen compounds.[18]

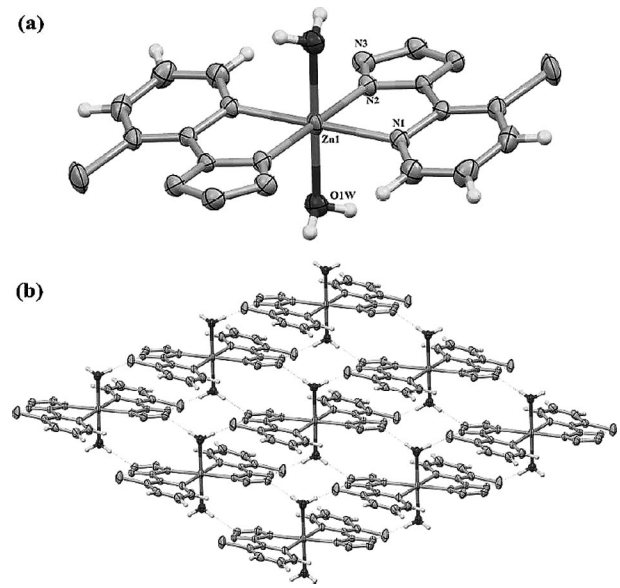

Figure 2. (a) Coordination environment of the Zn^{II} ion in compound **2**. (b) Hydrogen bonding in compound **2**.

As found in this work, the L1 ligand is nonplanar, with an average dihedral angle between the tetrazol ring and the benzene ring of 13.97°.[19] Each zinc unit is interconnected by four others by strong O–H···N hydrogen bonding, which come from coordinated water molecules and nitrogen atoms of L1 ligands, forming a 2D layer structure (Figure 2b). The intramolecular Cl···O halogen bonds between chlorine atoms and oxygen atoms of carboxylate group stabilized the layer structure and the adjacent layer is connected by non-classical C–H···C hydrogen bonds resulting in the final 3D supramolecular framework.

2.3 Crystal Structure of $[Cu(L2)_2]_n$ (3)

When HCl and $Cu(NO_3)_2{\cdot}6H_2O$ were added into the reaction, complex **3** was obtained in a good yield. X-ray single crystal diffraction indicates that complex **3** crystallizes in the monoclinic $P2_1/c$ space group. The fundamental structural unit of **3** contains one six-coordinate central copper(II) atom and a bridging L2 ligand. Each central Cu^{II} atom is located in an enlarged octahedron arrangement, bonded with two pyridine nitrogen donors and four oxygen donors of two L2 ligands. The Cu–N [1.963(2) Å] and Cu–O2 [1.935(2) Å] distances all fall into the normal bond length, but the Cu–O1 distances [2.650(4)] are longer than the normal bond length.[20] As shown in Figure 3, each central Cu^{II} ion links two neighboring Cu^{II} ions by four bridging L2 molecules, forming the 1D single chain structure. The nearest Cu···Cu distances are 4.9679(11) Å.

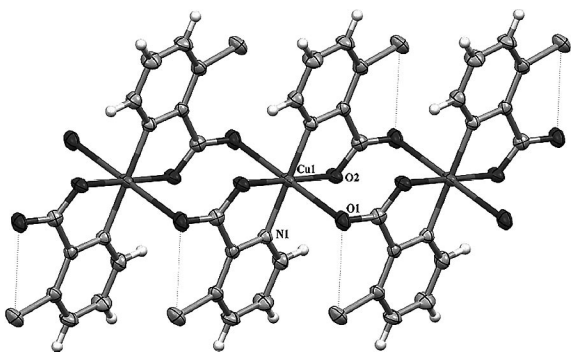

Figure 3. 1D chain of complex **3** along [0 1 0] direction.

2.4 Comparison of the Crystal Structures

X-ray crystallography revealed that the tetrazole-based ligand was generated in compounds **1** and **2**. For compound **3**, which is based on carboxylate ligands, the ligand was generated *in situ* from 3-chloro-2-cyanopyridine (Figure 4). From structural descriptions above, we can conclude that the structural nature of ligands have a remarkable impact on the frameworks of the compounds. In **1**, the L1 ligand adopted bidentate-chelate and monodentate coordination mode. In **2**, the L1 ligand only adopted bidentate-chelate coordination mode and the coordinated water molecules in each Zn^{2+} ion prevent its further extension to form high-dimensional framework. However, in **3**, the carboxylate groups connect Cu^{2+} ions to generate an infinite chain. For complex **1**, the two layers are interacted together through layer-to-layer hydrogen-bonding to generate a 3D supramolecular architecture and in **2**, strong O–H···N hydrogen bondings connected the 0D cluster to form a 2D layer.

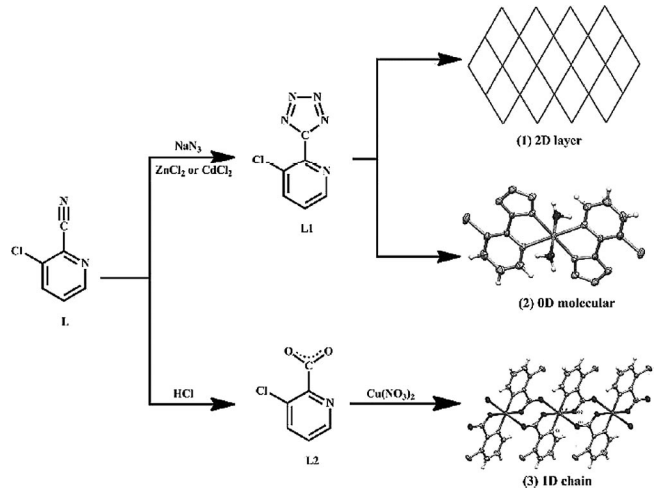

Figure 4. Structural diversities in compounds **1**–**3**.

Besides the structural nature of ligands, halogen bonds may be also playing some important role in the dimensionality of respective complexes. In complex **1**, the halogen bond between chlorine atoms and nitrogen atoms changed the 2D layer into a 3D net, whereas in complex **3** the intramolecular Cl···O halogen bonds between chlorine atoms and oxygen atoms of carboxylate group existed and also stabilized the 1D chain structure. For compound **2**, the nearest distance of Cl···O is 3.4 Å and there are no halogen bonds between chlorine atoms and oxygen atoms but for the two chlorine atoms belonging to the two different SBU the halogen bonds really exist between them, additionally stabilizing the layer structure

2.5 IR Spectra, Powder X-ray Diffraction Patterns, and Thermal Analysis

The as-synthesized samples of **1**, **2**, and **3** are air-stable and insoluble in water and common organic solvents, such as CH_3OH, C_2H_5OH. The IR spectra of compounds **1**–**3** (Figure S1, Supporting Information) show bands in the region of 1141–1491 cm^{-1}, which are attributed to characteristic peaks of the bipy group. Peaks appearing at 1600–1400 cm^{-1} should be assigned to stretching vibrations of the C=N bonds in imidazole rings in **1** and **2**. The IR spectrum of compound **2** shows a broad peak at 3500 cm^{-1} attributed to the O–H stretching vibration of the coordinated water molecules and the sharp bands in the ranges of 1700–1600 cm^{-1} and 1400–1300 cm^{-1} in **3** are attributed to asymmetric and symmetric stretching vibrations of the carboxylic group, respectively.

The powder X-ray diffraction (PXRD) patterns of the three compounds were also investigated at room temperature. As shown in Figure S2 (Supporting Information), all the PXRD patterns measured for the as-synthesized samples were in good

Zeitschrift für anorganische und allgemeine Chemie ZAAC Journal of Inorganic and General Chemistry

agreement with the PXRD patterns simulated from the respective single-crystal X-ray data using the Mercury 1.4 program, demonstrating the phase purity of the product. The dissimilarities in intensity may be due to the preferred orientation of the crystalline powder samples.[21]

The TG analyses of the compounds were examined in a nitrogen atmosphere in the temperature range of 30–800 °C with a heating rate of 10 °C·min^{-1}. As shown in Figure S3, the TGA curve of **1** showed a weight loss of 8.03% at 195–305 °C, which corresponds to the loss of lattice H_2O molecules. A sharp weight loss was found at 370 °C, corresponding to the decomposition of L1 ligand. The TGA curve of **2** displays a weight loss of 9.65% at 30–250 °C, which corresponds to the loss of coordinated and lattice H_2O molecules. Then, the compound began to decompose as the temperature was further increased. The TGA curve of complex **3** shows that the complex **3** is stable up to 276 °C, and the compound starts to decompose as the temperature was further increased.[22]

2.6 Photoluminescence Properties

Because of luminescent properties of d^{10} transition metals and their various applications in chemical sensors, photochemistry, and electroluminescent display, luminescence coordinated compounds are of great current interest.[23] Thus, the photoluminescence spectrum of **1** and **2** were investigated intensively in room temperature. Photoluminescence measurements for **1** and **2** show that they exhibit strong luminescence at λ_{max} = 348 and 380 nm, upon excitation at 275 and 285 nm (Figure 5). These emissions are neither metal-to-ligand charge transfer nor ligand-to-metal charge transfer. It can be assumed that these peaks derive from the n–π* transitions of the tetrazole ring,[24] because the Cd^{II} ion and Zn^{II} ion are difficult to oxidize or to reduce due to its d^{10} electronic configuration.[25] Compared with complex **2**, a red shift of 32 nm for **1** is observed, which is considered to originate from the influence of the coordination of the ligand to the central metal atoms.[26]

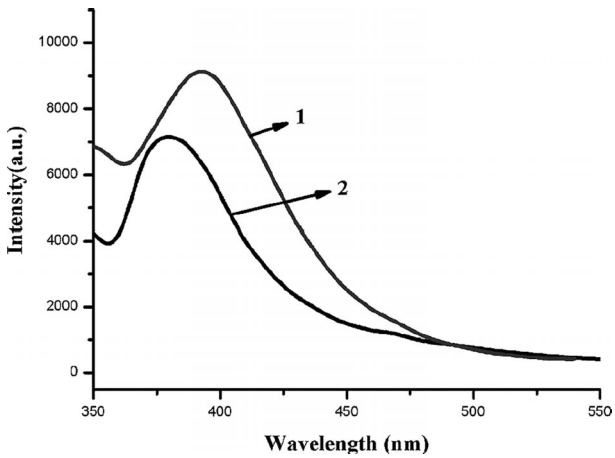

Figure 5. Emission spectra of compounds **1** and **2** measured in the solid state at room temperature.

3 Conclusions

Three metal organic coordination compounds based on carboxylate and tetrazolate ligands were synthesized by *in situ* ligand reaction from the same precursor and their crystal structures were characterized. They show diverse structures by changing from a zero-dimensional cluster to 1D chain to 2D 4^4 layer architecture. The changes of structure result from the different bridging abilities of carboxylate and tetrazolate ligands. Weak interactions, such as hydrogen bonds and halogen bonds, play an important role in the construction. In addition, such complexes display modest thermal stability and compound **1** and **2** show strong solid-state fluorescent emissions.

4 Experimental Sections

4.1 Materials and Equipments

All the starting materials used were commercially available and used without further purification. Powder X-ray diffraction measurements were finished with a Bruker AXS D8 Advance to check the phase purity. Elemental analyses (for C, H, and N) were carried out with a PerkinElmer 240 elemental analyzer. The FT-IR spectra were recorded in the range 4000–400 cm^{-1} with a Bruker VERTEX-70 spectrometer using the KBr pellet method. Thermogravimetric analysis (TGA) experiments were performed with a PerkinElmer TGA 7 instrument (heating rate of 10 °C·min^{-1}; nitrogen stream). Photoluminescence spectra were measured with a F-280 fluorescence spectrophotometer (slit width = 5 nm; sensitivity, high).

4.2 Synthesis of Compounds 1–3

$\{[Cd_2(L1)_4]_2 \cdot 9H_2O\}_n$ (1): A mixture of 3-chloro-2-cyanopyridine (5 mg, 0.04 mmol), $CdCl_2$ (20 mg, 0.15 mmol) and NaN_3 (10 mg, 0.15 mmol) was suspended in the solution (8 mL) of H_2O. A colorless solution was formed, which was heated in a teflon-lined steel bomb at 130 °C for 2 d. Yield: ca. 36% based on Cd. $C_{48}H_{42}Cd_4N_{40}O_9$: calcd. C 32.54, H 2.37, N 31.64%; found: C 32.57, H. 2.40, N 31.68%. **IR** (KBr, selected peaks): $\tilde{\nu}$ = 3067 (m), 1611 (s), 1491 (s), 1441 (vs), 1402 (vs), 1368 (s), 1238 (m), 1165 (m), 1082 (m), 1051 (m), 1021 (w), 816 (m), 770 (w), 726 (m), 661 (m), 515 (s), 452 (m) cm^{-1}.

$\{[Zn(L1)_2 \cdot 2H_2O]_2 \cdot H_2O\}_n$ (2): A similar procedure as for the preparation of **1** was applied except that the $CdCl_2$ was replaced by $ZnCl_2$. Colorless crystals of **2** were obtained in 39% yield based on Zn. $C_{24}H_{16}Zn_2N_{20}O$: calcd. C 39.40, H 2.19, N 38.30%.; found: C 39.38, H. 2.21, N 38.32%. **IR** (KBr, selected peaks): $\tilde{\nu}$ = 3342 (m), 1651 (w), 1591 (m), 1504 (m), 1447 (vs), 1415 (vs), 1372 (m), 1248 (m), 1207 (w), 1141 (m), 1088 (s), 1059 (m), 1038 (m), 1020 (w), 810 (m), 724 (s), 672 (m) cm^{-1}.

$[Cu(L2)_2]_n$ (3): A mixture of $Cu(NO_3)_2 \cdot 6H_2O$ (5 mg, 0.016 mmol) and 3-chloro-2-cyanopyridine (3 mg, 0.01 mmol) was suspended in the solution (1 mL) of H_2O. Afterwards a drop of hydrochloric acid was added into the solution and sealed in a pressure-resistant glass tube, slowly heated to 120 °C from room temperature in 500 min, kept at 120 °C for 3000 min, and then slowly cooled to 30 °C in 800 min. The blue rod crystals were collected and dried in air. Yield: ca. 33% based on Cu. Elemental analysis: calcd. C 38.04, H 2.11, N 7.40%; found: C 38.09, H. 2.09, N 7.42%. **IR** (KBr, selected peaks): $\tilde{\nu}$ = 3074 (m), 1648 (vs), 1577 (m), 1432 (s), 1335 (vs), 1254 (s), 1144 (m), 1085 (vs), 859 (s), 812 (s), 778 (w), 683 (m), 491 (m), 394 (w) cm^{-1}.

4.3. X-ray Crystallography

X-ray Crystallography Diffraction data for compounds **1**–**3** were collected with a Bruker APEX II CCD single-crystal X-ray diffractometer with a graphite-monochromated Mo-K_α radiation (λ = 0.71073 Å) source at 298 K. All absorption corrections were applied using the multi-scan program SADABS. In these cases, the highest possible space group was chosen. All structures were solved by direct methods using the SHELXS-97[27] program of the SHELXTL package and refined by the full-matrix least-squares method with SHELXL-97.[28] All non-hydrogen atoms in the three structures were refined on F^2 with anisotropic displacement parameters. Crystal structure pictures were obtained using Diamond v3.1f and ChemDraw. Crystallographic data and experimental details for structural analyses for **1**–**3** are summarized in Table S1 (Supporting Information), and selected bond lengths and bond angles are listed in Table S2–S4 (Supporting Information).

Supporting Information (see footnote on the first page of this article): The PXRD patterns, TGA curves, IR spectra, and crystal data of compounds **1**–**3**.

Acknowledgements

This work was supported by the National Natural Science Foundation of China (Grant No. 21271117), NCET-11–0309 and the Shandong Natural Science Fund for Distinguished Young Scholars (JQ201003), Natural Science Foundation of Shandong Province (ZR2010BL011, BS2011CL041), and the Fundamental Research Funds for the Central Universities (13CX05010A).

References

[1] a) C. M. G. dos Santos, A. J. Harte, S. J. Quinn, T. Gunnlaugsson, *Coord. Chem. Rev.* **2008**, *252*, 2512–2527; b) P. Wang, J. P. Ma, Y. B. Dong, R. Q. Huang, *J. Am. Chem. Soc.* **2007**, *129*, 10620–10621; c) P. K. Thallapally, J. Tian, R. K. Motkuri, C. A. Fernandez, S. J. Dalgarno, P. B. McGrail, J. E. Warren, J. L. Atwood, *J. Am. Chem. Soc.* **2008**, *130*, 16842–16843.

[2] a) P. Lebduskova, P. Hermann, L. Helm, E. Toth, J. Kotek, K. Binnemans, J. Rudovsky, I. Lukes, A. E. Merbach, *Dalton Trans.* **2007**, *4*, 493–501; b) B. Moulton, M. J. Zaworotko, *Chem. Rev.* **2001**, *101*, 1629–1658; c) X. Y. Chen, Y. Bretonnière, J. Pécaut, D. Imbert, J. C. G. Bünzli, M. Mazzanti, *Inorg. Chem.* **2007**, *46*, 625–637.

[3] a) B. Zhao, P. Cheng, X. Y. Chen, C. Cheng, W. Shi, D. Z. Liao, S. P. Yan, Z. H. Jiang, *J. Am. Chem. Soc.* **2004**, *126*, 3012–3013; b) C. A. Fernandez, P. K. Thallapally, M. R. Kishan, S. K. Nune, J. Liu, B. P. McGrail, *Cryst. Growth Des.* **2010**, *10*, 1037–1039; c) R. K. Motkuri, J. Tian, P. K. Thallaphally, C. A. Fernandez, P. B. McGrail, *Chem. Commun.* **2010**, *46*, 538–540.

[4] a) T. Wu, B. H. Yi, D. Li, *Inorg. Chem.* **2005**, *44*, 4130–4132; b) T. Wu, R. Zhou, D. Li, *Inorg. Chem. Commun.* **2006**, *9*, 341–345.

[5] a) X. M. Zhang, Y. F. Zhao, H. S. Wu, S. R. Batten, S. W. Ng, *Dalton Trans.* **2006**, *26*, 3170–3178; b) J. J. Hou, Z. M. Hao, X. M. Zhang, *Inorg. Chim. Acta* **2007**, *360*, 14–20.

[6] J. Tao, Z. J. Ma, R. B. Huang, L. S. Zheng, *Inorg. Chem.* **2004**, *43*, 6133–6135.

[7] X. He, C. Z. Lu, D. Q. Yuan, *Inorg. Chem.* **2006**, *45*, 5760–5766.

[8] W. Wei, M. Y. Wu, Q. Gao, Q. F. Zhang, Y. G. Huang, F. L. Jiang, M. C. Hong, *Inorg. Chem.* **2009**, *48*, 420–422.

[9] J. Y. Wu, S. M. Huang, Y. C. Huang, K. L. Lu, *CrystEngComm* **2012**, *14*, 1189–1192.

[10] Z. F. Liu, M. F. Wu, F. K. Zheng, S. H. Wang, M. J. Zhang, J. Chen, Y. Xiao, G. C. Guo, A. Q. Wu, *CrystEngComm* **2013**, *15*, 7038–7047.

[11] T. P. Hu, W. H. Bi, X. Q. Hu, X. L. Zhao, D. F. Sun, *Cryst. Growth Des.* **2010**, *10*, 3324–3326.

[12] J. B. Tan, X. Y. Chen, J. Fan, S. R. Zheng, W. G. Zhang, *Inorg. Chem. Commun.* **2013**, *31*, 49–53.

[13] O. Takahashi, Y. J. Kohno, M. Nishi, *Chem. Rev.* **2010**, *110*, 6049–6076.

[14] a) Z. P. Demko, K. B. Sharpless, *JOC* **2001**, *66*, 7945–7950; b) Z. P. Demko, K. B. Sharpless, *Org. Lett.* **2001**, *3*, 4091–4094; c) Z. P. Demko, K. B. Sharpless, *Org. Lett.* **2002**, *4*, 2525–2527; d) F. Himo, Z. P. Demko, L. Noodleman, K. B. Sharpless, *J. Am. Chem. Soc.* **2001**, *123,* 12210–12216.

[15] C. C. Chang, Y. C. Huang, S. M. Huang, J. Y. Wu, Y. H. Liu, K. L. Lu, *Cryst. Growth Des.* **2012**, *12*, 3825–3828.

[16] O. V. Dolomanov, L. J. Bourhis, R. J. Gildea, J. A. K. Howard, H. Puschmann, *J. Appl. Crystallogr.* **2009**, *42*, 339.

[17] L. L. Zhang, F. L. Liu, Y. Guo, X. P. Wang, J. Guo, Y. H. Wei, Z. Chen, D. F. Sun, *Cryst. Growth Des.* **2012**, *12*, 6215–6222.

[18] H. B. Zhu, W. N. Yang, J. Hu, *J. Coord. Chem.* **2013**, *16*, 2775–2787.

[19] D. K. Kumar, D. A. Jose, A. Das, P. Dastidar, *Inorg. Chem.* **2005**, *44*, 6933–6935.

[20] S. Mohapatra, H. Sato, R. Matsuda, S. Kitagawa, T. K. Maji, *CrystEngComm* **2012**, *14*, 4153–4156.

[21] X. L. Zhao, S. N. Wang, X. Y. Wang, J. M. Dou, P. P. Cui, Z. Chen, D. Sun, X. P. Wang, D. F. Sun, *Cryst. Growth Des.* **2012**, *12*, 2736–2739.

[22] J. Guo, L. L. Zhang, H. Q. Ma, Z. Chen, D. I. Sun, Y. H. Wei, D. F. Sun, *Inorg. Chem. Commun.* **2013**, *28*, 75–80.

[23] V. W. Yam, K. K. W. Lo, *Chem. Soc. Rev.* **1999**, *28*, 323–334.

[24] Y. B. Wang, D. S. Liu, T. H. Pan, Q. Liang, X. H. Huang, S. T. Wu, C. C. Huang, *CrystEngComm* **2010**, *12*, 3886–3893.

[25] C. C. Ji, L. Qin, Y. Z. Li, Z. J. Guo, H. G. Zheng, *Cryst. Growth Des.* **2011**, *11*, 480–487.

[26] a) L. Wen, Z. Lu, J. Lin, Z. Tian, H. Zhu, Q. Meng, *Cryst. Growth Des.* **2007**, *7*, 93–99; b) J. G. Lin, S. Q. Zang, Z. F. Tian, Y. Z. Li, Y. Y. Xu, H. Z. Zhu, Q. J. Meng, *CrystEngComm* **2007**, *9*, 915–921; c) L. Wen, Y. Li, Z. Lu, J. Lin, C. Duan, Q. Meng, *Cryst. Growth Des.* **2006**, *6*, 530–537.

[27] G. M. Sheldrick, *SHELXS-97*, Program for X-ray Crystal Structure Determination, University of Göttingen, Germany, **1997**.

[28] G. M. Sheldrick, *SHELXL-97*, Program for X-ray Crystal Structure Refinement, University of Göttingen, Germany, **1997**.

Received: December 11, 2013
Published Online: February 12, 2014

